

# THE BEHAVIOUR OF THE GAUSS-RADAU UPPER BOUND OF THE ERROR NORM IN CG\*

GÉRARD MEURANT<sup>†</sup> AND PETR TICHÝ<sup>‡</sup>

September 30, 2022

**Abstract.** Consider the problem of solving systems of linear algebraic equations  $Ax = b$  with a real symmetric positive definite matrix  $A$  using the conjugate gradient (CG) method. To stop the algorithm at the appropriate moment, it is important to monitor the quality of the approximate solution  $x_k$ . One of the most relevant quantities for measuring the quality of  $x_k$  is the  $A$ -norm of the error. This quantity cannot be easily evaluated, however, it can be estimated. In this paper we discuss and analyze the behaviour of the Gauss-Radau upper bound on the  $A$ -norm of the error, based on viewing CG as a procedure for approximating a certain Riemann-Stieltjes integral. This upper bound depends on a prescribed underestimate  $\mu$  to the smallest eigenvalue of  $A$ . We concentrate on explaining a phenomenon observed during computations showing that, in later CG iterations, the upper bound loses its accuracy, and it is almost independent of  $\mu$ . We construct a model problem that is used to demonstrate and study the behaviour of the upper bound in dependence of  $\mu$ , and developed formulas that are helpful in understanding this behavior. We show that the above mentioned phenomenon is closely related to the convergence of the smallest Ritz value to the smallest eigenvalue of  $A$ . It occurs when the smallest Ritz value is a better approximation to the smallest eigenvalue than the prescribed underestimate  $\mu$ . We also suggest an adaptive strategy for improving the accuracy of the Gauss-Radau upper bound such that the resulting estimate approximates the quantity of interest with a prescribed relative accuracy.

**Key words.** Conjugate gradients, error bounds, Gauss-Radau quadrature

**AMS subject classifications.** 65F10, 65G50

**1. Introduction.** Our aim in this paper is to explain the origin of the problems that have been noticed [19] when using Gauss-Radau quadrature upper bounds of the  $A$ -norm of the error in the Conjugate Gradient (CG) algorithm for solving linear systems  $Ax = b$  with a symmetric positive definite matrix of order  $N$ .

The connection between CG and Gauss quadrature has been known since the seminal paper of Hestenes and Stiefel [11] in 1952. This link has been exploited by Gene H. Golub and his collaborators to bound or estimate the  $A$ -norm of the error in CG during the iterations; see [1, 2, 5, 6, 7, 12, 13, 17, 18, 19, 24, 25].

Using a fixed node  $\mu$  smaller than the smallest eigenvalue of  $A$  and the Gauss-Radau quadrature rule, an upper bound for the  $A$ -norm of the error can be easily computed. Note that it is useful to have an upper bound of the error norm to stop the CG iterations. In theory, the closer  $\mu$  is to the smallest eigenvalue, the closer is the bound to the norm. However, in many examples, even if the bound is close to the norm at the beginning of the CG iterations, the upper bound becomes worse after a while and almost independent of  $\mu$ , even in exact arithmetic. Therefore, this problem is not linked to rounding errors and has to be explained.

The Gauss quadrature bounds of the error norm were obtained by using the connection of CG to the Lanczos algorithm and modifications of the tridiagonal matrix which is generated by this algorithm and implicitly by CG. This is why we start in Section 2 with the Lanczos algorithm. In Section 3 we discuss the relation with CG

---

\*Version of September 30, 2022. The work of P. Tichý was supported by the Grant Agency of the Czech Republic under grant no. 20-01074S

<sup>†</sup>Paris, France. E-mail: [gerard.meurant@gmail.com](mailto:gerard.meurant@gmail.com).

<sup>‡</sup>Faculty of Mathematics and Physics, Charles University, Prague, Czech Republic. E-mail: [petr.tichy@mff.cuni.cz](mailto:petr.tichy@mff.cuni.cz).

and how the Gauss-Radau upper bound is computed. A model problem showing the problems arising with the Gauss-Radau bound in “exact” arithmetic is constructed in Section 4. In Sections 5 to 7 we give an analysis that explains that the problems start when the distance of the smallest Ritz value to the smallest eigenvalue becomes smaller than the distance of  $\mu$  to the smallest eigenvalue. We also explain why the Gauss-Radau upper bound becomes almost independent of  $\mu$ . In Section 8 we give an algorithm for improving the accuracy of the upper bound at iteration  $k$  using the information from the next CG iterations. In particular, the algorithm determines adaptively the number of forthcoming CG iterations that are needed to get an estimate with a prescribed relative accuracy. Conclusions are given in Section 9.

**2. The Lanczos algorithm.** Given a starting vector  $v$  and a symmetric matrix  $A \in \mathbb{R}^{N \times N}$ , one can consider a sequence of nested Krylov subspaces

$$\mathcal{K}_k(A, v) \equiv \text{span}\{v, Av, \dots, A^{k-1}v\}, \quad k = 1, 2, \dots$$

The dimension of these subspaces can increase up to an index  $n$  called the *grade of  $v$  with respect to  $A$* , at which the maximal dimension is attained, and  $\mathcal{K}_n(A, v)$  is invariant under multiplication with  $A$ .

---

**Algorithm 1** Lanczos algorithm

---

**input**  $A, v$   
 $\beta_0 = 0, v_0 = 0$   
 $v_1 = v/\|v\|$   
**for**  $k = 1, \dots$  **do**  
 $w = Av_k - \beta_{k-1}v_{k-1}$   
 $\alpha_k = v_k^T w$   
 $w = w - \alpha_k v_k$   
 $\beta_k = \|w\|$   
 $v_{k+1} = w/\beta_k$   
**end for**

---

Assuming that  $k < n$ , the Lanczos algorithm (Algorithm 1) computes an orthonormal basis  $v_1, \dots, v_{k+1}$  of the Krylov subspace  $\mathcal{K}_{k+1}(A, v)$ . The basis vectors  $v_j$  satisfy the matrix relation

$$AV_k = V_k T_k + \beta_k v_{k+1} e_k^T$$

where  $e_k$  is the last column of the identity matrix of order  $k$ ,  $V_k = [v_1 \cdots v_k]$  and  $T_k$  is the  $k \times k$  symmetric tridiagonal matrix of the recurrence coefficients computed in Algorithm 1:

$$T_k = \begin{bmatrix} \alpha_1 & \beta_1 & & & \\ \beta_1 & \ddots & \ddots & & \\ & \ddots & \ddots & \beta_{k-1} & \\ & & \beta_{k-1} & \alpha_k & \end{bmatrix}.$$

The coefficients  $\beta_j$  being positive,  $T_k$  is a so-called Jacobi matrix. If  $A$  is positive definite, then  $T_k$  is positive definite as well. In the following we will assume for simplicity that the eigenvalues of  $A$  are simple and sorted such that

$$\lambda_1 < \lambda_2 < \cdots < \lambda_N.$$

**2.1. Approximation of the eigenvalues.** The eigenvalues of  $T_k$  (Ritz values) are usually used as approximations to the eigenvalues of  $A$ . The quality of the approximation can be measured using  $\beta_k$  and the last components of the normalized eigenvectors of  $T_k$ . In more detail, consider the spectral decomposition of  $T_k$  in the form

$$T_k = S_k \Theta_k S_k^T, \quad \Theta_k = \text{diag} \left( \theta_1^{(k)}, \dots, \theta_k^{(k)} \right), \quad S_k^T S_k = S_k S_k^T = I_k,$$

where  $I_k$  is the identity matrix of order  $k$ , and assume that the Ritz values are sorted such that

$$\theta_1^{(k)} < \theta_2^{(k)} < \dots < \theta_k^{(k)}.$$

Denote  $s_{i,j}^{(k)}$  the entries and  $s_{:,j}^{(k)}$  the columns of  $S_k$ . Then it holds that

$$(2.1) \quad \min_{i=1, \dots, N} |\lambda_i - \theta_j^{(k)}| \leq \left\| A \left( V_k s_{:,j}^{(k)} \right) - \theta_j^{(k)} \left( V_k s_{:,j}^{(k)} \right) \right\| = \beta_k \left| s_{k,j}^{(k)} \right|,$$

$j = 1, \dots, k$ . Since the Ritz values  $\theta_j^{(k)}$  can be seen as Rayleigh quotients, one can improve the bound (2.1) using the gap theorem; see [22, p. 244] or [3, p. 206]. In particular, let  $\lambda_\ell$  be an eigenvalue of  $A$  closest to  $\theta_j^{(k)}$ . Then

$$|\lambda_\ell - \theta_j^{(k)}| \leq \frac{\left( \beta_k s_{k,j}^{(k)} \right)^2}{\text{gap}_j^{(k)}}, \quad \text{gap}_j^{(k)} = \min_{i \neq \ell} \left| \lambda_i - \theta_j^{(k)} \right|.$$

In the following we will be interested in the situation when the smallest Ritz value  $\theta_1^{(k)}$  closely approximates the smallest eigenvalue of  $A$ . If  $\lambda_1$  is the eigenvalue of  $A$  closest to  $\theta_1^{(k)} > \lambda_1$ , then using the gap theorem and [22, Corollary 11.7.1 on p. 246],

$$(2.2) \quad \frac{\left( \beta_k s_{k,1}^{(k)} \right)^2}{\lambda_n - \lambda_1} \leq \theta_1^{(k)} - \lambda_1 \leq \frac{\left( \beta_k s_{k,1}^{(k)} \right)^2}{\lambda_2 - \theta_1^{(k)}},$$

giving the bounds

$$(2.3) \quad \lambda_2 - \theta_1^{(k)} \leq \frac{\left( \beta_k s_{k,1}^{(k)} \right)^2}{\theta_1^{(k)} - \lambda_1} \leq \lambda_n - \lambda_1.$$

It is known (see, for instance, [14]) that the squares of the last components of the eigenvectors are given by

$$\left( s_{k,j}^{(k)} \right)^2 = \left| \frac{\chi_{1,k-1}(\theta_j^{(k)})}{\chi'_{1,k}(\theta_j^{(k)})} \right|,$$

where  $\chi_{1,\ell}$  is the characteristic polynomial of  $T_\ell$  and  $\chi'_{1,\ell}$  denotes its derivative, i.e.,

$$\left( s_{k,j}^{(k)} \right)^2 = \frac{\theta_j^{(k)} - \theta_1^{(k-1)}}{\theta_j^{(k)} - \theta_1^{(k)}} \cdots \frac{\theta_j^{(k)} - \theta_{j-1}^{(k-1)}}{\theta_j^{(k)} - \theta_{j-1}^{(k)}} \frac{\theta_j^{(k-1)} - \theta_j^{(k)}}{\theta_{j+1}^{(k)} - \theta_j^{(k)}} \cdots \frac{\theta_{k-1}^{(k-1)} - \theta_j^{(k)}}{\theta_k^{(k)} - \theta_j^{(k)}}.$$

The right-hand side is positive due to the interlacing property of the Ritz values for symmetric tridiagonal matrices. In particular,

$$(2.4) \quad \left(s_{k,1}^{(k)}\right)^2 = \frac{\theta_1^{(k-1)} - \theta_1^{(k)}}{\theta_2^{(k)} - \theta_1^{(k)}} \cdots \frac{\theta_{k-1}^{(k-1)} - \theta_1^{(k)}}{\theta_k^{(k)} - \theta_1^{(k)}}.$$

When the smallest Ritz value  $\theta_1^{(k)}$  converges to  $\lambda_1$ , this last component squared converges to zero; see also (2.3).

**2.2. Modification of the tridiagonal matrix.** The nodes of the Gauss quadrature are given by the eigenvalues of  $T_k$ . To obtain the Gauss-Radau quadrature rule one has to consider the problem of finding the coefficient  $\alpha_{k+1}^{(\mu)}$  such that the modified matrix

$$(2.5) \quad T_{k+1}^{(\mu)} = \begin{bmatrix} \alpha_1 & \beta_1 & & & & \\ \beta_1 & \ddots & \ddots & & & \\ & \ddots & \ddots & \beta_{k-1} & & \\ & & \beta_{k-1} & \alpha_k & \beta_k & \\ & & & \beta_k & \alpha_{k+1}^{(\mu)} & \end{bmatrix}$$

has the prescribed  $\mu$  as an eigenvalue. The nodes of the Gauss-Radau quadrature rule are the eigenvalues of this matrix and the weights are obtained from its eigenvectors. In [4, pp. 331-334] it has been shown that at iteration  $k + 1$

$$\alpha_{k+1}^{(\mu)} = \mu + \zeta_k^{(\mu)}$$

where  $\zeta_k^{(\mu)}$  is the last component of the vector  $y$  that solves the linear system

$$(2.6) \quad (T_k - \mu I)y = \beta_k^2 e_k.$$

From [17, Section 3.4], the modified coefficients  $\alpha_{k+1}^{(\mu)}$  can be computed recursively using

$$(2.7) \quad \alpha_{j+1}^{(\mu)} = \mu + \frac{\beta_j^2}{\alpha_j - \alpha_j^{(\mu)}}, \quad \alpha_1^{(\mu)} = \mu, \quad j = 1, \dots, k.$$

Based on the spectral factorization of  $T_k$ , we can now prove the following lemma.

LEMMA 2.1. *Let  $\mu < \theta_1^{(k)}$ . Then it holds that*

$$(2.8) \quad \alpha_{k+1}^{(\mu)} = \mu + \sum_{i=1}^k \eta_{i,k}^{(\mu)}, \quad \eta_{i,k}^{(\mu)} \equiv \frac{\left(\beta_k s_{k,i}^{(k)}\right)^2}{\theta_i^{(k)} - \mu}.$$

*If  $\mu < \lambda < \theta_1^{(k)}$ , then  $\alpha_{k+1}^{(\mu)} < \alpha_{k+1}^{(\lambda)}$ . Consequently, if  $\mu < \theta_1^{(k+1)}$ , then  $\alpha_{k+1}^{(\mu)} < \alpha_{k+1}$ .*

*Proof.* Since  $\mu < \theta_1^{(k)}$  the matrix  $T_k - \mu I$  in (2.6) is positive definite and, therefore, nonsingular. Hence,

$$(2.9) \quad \zeta_k^{(\mu)} = e_k^T y = \beta_k^2 e_k^T (T_k - \mu I)^{-1} e_k = \sum_{i=1}^k \frac{\left(\beta_k s_{k,i}^{(k)}\right)^2}{\theta_i^{(k)} - \mu}$$

so that (2.8) holds.

From (2.8) it is obvious that if  $\mu < \lambda < \theta_1^{(k)}$ , then  $\alpha_{k+1}^{(\mu)} < \alpha_{k+1}^{(\lambda)}$ . Finally, taking  $\lambda = \theta_1^{(k+1)} < \theta_1^{(k)}$  (because of the interlacing of the Ritz values) we obtain

$$(2.10) \quad \alpha_{k+1}^{(\lambda)} = \alpha_{k+1} = \theta_1^{(k+1)} + \zeta_k, \quad \zeta_k = \sum_{i=1}^k \frac{(\beta_k s_{k,i}^{(k)})^2}{\theta_i^{(k)} - \theta_1^{(k+1)}}.$$

If  $\mu < \theta_1^{(k+1)} = \lambda$ , then  $\alpha_{k+1}^{(\mu)} < \alpha_{k+1}^{(\lambda)} = \alpha_{k+1}$ .  $\square$

**3. The conjugate gradient method and error norm estimation.** When solving a linear system  $Ax = b$  with a symmetric and positive definite matrix  $A$ , the CG method (Algorithm 2) is the method of choice. In exact arithmetic, the CG

---

**Algorithm 2** Conjugate gradient algorithm

---

```

input  $A, b, x_0$ 
 $r_0 = b - Ax_0$ 
 $p_0 = r_0$ 
for  $k = 1, \dots$  until convergence do
   $\gamma_{k-1} = \frac{r_{k-1}^T r_{k-1}}{p_{k-1}^T A p_{k-1}}$ 
   $x_k = x_{k-1} + \gamma_{k-1} p_{k-1}$ 
   $r_k = r_{k-1} - \gamma_{k-1} A p_{k-1}$ 
   $\delta_k = \frac{r_k^T r_k}{r_{k-1}^T r_{k-1}}$ 
   $p_k = r_k + \delta_k p_{k-1}$ 
} cgiter(k-1)
end for

```

---

iterates  $x_k$  minimize the  $A$ -norm of the error over the manifold  $x_0 + \mathcal{K}_k(A, r_0)$ ,

$$\|x - x_k\|_A = \min_{y \in x_0 + \mathcal{K}_k(A, r_0)} \|x - y\|_A,$$

and the residual vectors  $r_k = b - Ax_k$  are proportional to the Lanczos vectors  $v_j$ ,

$$v_{j+1} = (-1)^j \frac{r_j}{\|r_j\|}, \quad j = 0, \dots, k.$$

Thanks to this close relationship between the CG and Lanczos algorithms it can be shown (see, for instance [14]) that the recurrence coefficients computed in both algorithms are connected via  $\alpha_1 = \gamma_0^{-1}$  and

$$(3.1) \quad \beta_j = \frac{\sqrt{\delta_j}}{\gamma_{j-1}}, \quad \alpha_{j+1} = \frac{1}{\gamma_j} + \frac{\delta_j}{\gamma_{j-1}}, \quad j = 1, \dots, k-1.$$

Writing (3.1) in matrix form, we find out that CG computes implicitly the  $LDL^T$  factorization  $T_k = L_k D_k L_k^T$ , where

$$(3.2) \quad L_k = \begin{bmatrix} 1 & & & & \\ \sqrt{\delta_1} & \ddots & & & \\ & \ddots & \ddots & & \\ & & \ddots & \ddots & \\ & & & \sqrt{\delta_{k-1}} & 1 \end{bmatrix}, \quad D_k = \begin{bmatrix} \gamma_0^{-1} & & & & \\ & \ddots & & & \\ & & \ddots & & \\ & & & \ddots & \\ & & & & \gamma_{k-1}^{-1} \end{bmatrix}.$$

Hence the matrix  $T_k$  is known implicitly in CG.

**3.1. Modification of the factorization of the tridiagonal matrix.** Similarly as in Section 2.2 we can ask how to modify the Cholesky factorization of  $T_{k+1}$ , that is available in CG, such that the resulting matrix  $T_{k+1}^{(\mu)}$  given implicitly in factorized form has the prescribed eigenvalue  $\mu$ . In more detail, we look for a coefficient  $\gamma_k^{(\mu)}$  such that

$$T_{k+1}^{(\mu)} = L_{k+1} \begin{bmatrix} D_k & \\ & (\gamma_k^{(\mu)})^{-1} \end{bmatrix} L_{k+1}^T.$$

This problem was solved in [17] leading to an updating formula for computing the modified coefficients

$$(3.3) \quad \gamma_{j+1}^{(\mu)} = \frac{\gamma_j^{(\mu)} - \gamma_j}{\mu(\gamma_j^{(\mu)} - \gamma_j) + \delta_{j+1}}, \quad j = 1, \dots, k-1, \quad \gamma_0^{(\mu)} = \frac{1}{\mu}.$$

Moreover,  $\gamma_k^{(\mu)}$  can be obtained directly from the modified coefficient  $\alpha_{k+1}^{(\mu)}$ ,

$$(3.4) \quad \gamma_k^{(\mu)} = \frac{1}{\alpha_{k+1}^{(\mu)} - \frac{\delta_k}{\gamma_{k-1}}},$$

and vice-versa, see [17, p. 173 and 181].

**3.2. The Gauss-Radau upper bound.** To summarize some results of [5, 7, 24], and [17, 18, 19] related to the Gauss and Gauss-Radau quadrature bounds for the  $A$ -norm of the error in CG, it has been shown that

$$(3.5) \quad \gamma_k \|r_k\|^2 \leq \|x - x_k\|_A^2 < \gamma_k^{(\mu)} \|r_k\|^2 < \left( \frac{\|r_k\|^2}{\mu \|p_k\|^2} \right) \|r_k\|^2$$

for  $k < n-1$ , and  $\mu$  such that  $0 < \mu \leq \lambda_1$ . Note that in the special case  $k = n-1$  it holds that  $\|x - x_{n-1}\|_A^2 = \gamma_{n-1} \|r_{n-1}\|^2$ . If the initial residual  $r_0$  has a nontrivial component in the eigenvector corresponding to  $\lambda_1$ , then  $\lambda_1$  is an eigenvalue of  $T_n$ . If in addition  $\mu$  is chosen such that  $\mu = \lambda_1$ , then  $\gamma_{n-1} = \gamma_{n-1}^{(\mu)}$  and the second inequality in (3.5) changes to equality. The last inequality is strict also for  $k = n-1$ .

The rightmost bound in (3.5) was derived in [19]. The norm  $\|p_k\|$  is not available in CG, but the ratio

$$\phi_k = \frac{\|r_k\|^2}{\|p_k\|^2}$$

can be computed efficiently using

$$(3.6) \quad \phi_{j+1}^{-1} = 1 + \phi_j^{-1} \delta_{j+1}, \quad \phi_0 = 1.$$

Note that the accuracy of the bounds can be improved using the formula

$$(3.7) \quad \|x - x_k\|_A^2 = \sum_{j=k}^{\ell-1} \gamma_j \|r_k\|^2 + \|x - x_\ell\|_A^2$$

for a convenient positive integer  $\ell \geq k$ , by applying the basic bounds (3.5) to the last term in (3.7); see [19] for details on the construction of more accurate bounds. In

practice, however, one runs the CG algorithm, and estimates the error in a backward way, i.e.,  $\ell - k$  iterations back. The adaptive choice of the delay  $\ell - k$  when using the Gauss quadrature lower bound was discussed recently in [16].

In the following we will concentrate on the analysis of the behaviour of the basic Gauss-Radau upper bound (3.5) corresponding to  $\ell = k$

$$(3.8) \quad \gamma_k^{(\mu)} \|r_k\|^2$$

in dependence of the choice of  $\mu$ . As said above, in theory, the closer  $\mu$  is to  $\lambda_1$ , the closer to the  $A$ -norm of the error is the upper bound. However, this is not what is observed in many examples, even in exact arithmetic. In the next section, we construct a model problem and perform numerical experiments that will motivate our analysis.

**4. The model problem and a numerical experiment.** In the construction of the motivating example we use results presented in [9, 10, 14, 20, 23]. Based on the work by Chris Paige [21], Anne Greenbaum [9] proved that the results of finite precision CG computations can be interpreted (up to some small inaccuracies) as the results of the exact CG algorithm applied to a larger system with the system matrix having many eigenvalues distributed throughout “tiny” intervals around the eigenvalues of the original matrix. The experiments show that “tiny” means of the size comparable to  $\mathbf{u}\|A\|$ , where  $\mathbf{u}$  is the roundoff unit. This result was used in [10] to predict the behavior of finite precision CG. Inspired by [9, 10, 20] we will construct a linear system  $Ax = b$  with similar properties as the one suggested by Greenbaum [9]. However, we want to emphasize and visualize some phenomenons concerning the behaviour of the basic Gauss-Radau upper bound (3.8). Therefore, we choose the size of the intervals around the original eigenvalues larger than  $\mathbf{u}\|A\|$ .

We start with the test problem  $\Lambda y = w$  from [23], where  $w = m^{-1/2}(1, \dots, 1)^T$  and  $\Lambda = \text{diag}(\hat{\lambda}_1, \dots, \hat{\lambda}_m)$ ,

$$(4.1) \quad \hat{\lambda}_i = \hat{\lambda}_1 + \frac{i-1}{m-1}(\hat{\lambda}_m - \hat{\lambda}_1)\rho^{m-i}, \quad i = 2, \dots, m.$$

The diagonal matrix  $\Lambda$  and the vector  $w$  determine the stepwise distribution function  $\omega(\lambda)$  with points of increase  $\hat{\lambda}_i$  and the individual jumps (weights)  $\omega_j = m^{-1}$ ,

$$(4.2) \quad \omega(\lambda) \equiv \begin{cases} 0 & \text{for } \lambda < \hat{\lambda}_1, \\ \sum_{j=1}^i \omega_j & \text{for } \hat{\lambda}_i \leq \lambda < \hat{\lambda}_{i+1}, \quad 1 \leq i \leq m-1, \\ 1 & \text{for } \hat{\lambda}_m \leq \lambda. \end{cases}$$

We construct a blurred distribution function  $\tilde{\omega}(\lambda)$  having clusters of points of increase around the original eigenvalues  $\hat{\lambda}_i$ . We consider each cluster to have the same radius  $\delta$ , and let the number  $c_i$  of points in the  $i$ th cluster grow linearly from 1 to  $p$ ,

$$c_i = \text{round} \left( \frac{p-1}{m-1}i + \frac{m-p}{m-1} \right), \quad i = 1, \dots, m.$$

The blurred eigenvalues

$$\tilde{\lambda}_j^{(i)}, \quad j = 1, \dots, c_i,$$

are uniformly distributed in  $[\hat{\lambda}_i - \delta, \hat{\lambda}_i + \delta]$ , with the corresponding weights given by

$$\tilde{\omega}_j^{(i)} = \frac{\omega_i}{c_i} \quad j = 1, \dots, c_i,$$

i.e., the weights that correspond to the  $i$ th cluster are equal, and their sum is  $\omega_i$ . Having defined the blurred distribution function  $\tilde{\omega}(\lambda)$  we can construct the corresponding Jacobi matrix  $T \in \mathbb{R}^{N \times N}$  using the Gragg and Harrod rkpw algorithm [8].

To construct the above mentioned Jacobi matrix  $T$  we used Matlab's vpa arithmetic with 128 digits. Finally, we define the *double precision data*  $A$  and  $b$  that will be used for experimenting as

$$(4.3) \quad A = \text{double}(T), \quad b = e_1,$$

where  $e_1 \in \mathbb{R}^N$  is the first column of the identity matrix. We decided to use double precision input data from two reasons. First, we can easily compare results of our computations performed in Matlab's vpa arithmetic with results obtained using double precision arithmetic for the same input data. Second, the nonzero structure of the double precision input data allows us to exploit results of [26] showing that the Lanczos algorithm applied to  $A$  and  $b$  having the nonzero structure as in (4.3), computes exactly. Hence, if we want to simulate exact CG computations, then we can use [26, Algorithm 3], and not all computations have to be performed using the (slow) Matlab vpa arithmetic.

In our experiment we choose  $m = 12$ ,  $\hat{\lambda}_1 = 10^{-6}$ ,  $\hat{\lambda}_m = 1$ ,  $\rho = 0.8$ ,  $\delta = 10^{-10}$ , and  $p = 4$ , resulting in  $N = 30$ . Let us run the "exact" CGQ algorithm of [17] on the model problem (4.3) constructed above, where exact arithmetic is simulated using Matlab's variable precision with `digits=128`. Let  $\lambda_1$  be the exact smallest eigenvalue of  $A$ . We use four different values of  $\mu$  for the computation of the Gauss-Radau upper bound (3.8):  $\mu_3 = (1 - 10^{-3})\lambda_1$ ,  $\mu_8 = (1 - 10^{-8})\lambda_1$ ,  $\mu_{16}$  which denotes the double precision number closest to  $\lambda_1$  such that  $\mu_{16} \leq \lambda_1$ , and  $\mu_{50} = (1 - 10^{-50})\lambda_1$  which is almost like the exact value. Note that  $\gamma_k^{(\mu)}$  is updated using (3.3).

Figure 4.1 shows the  $A$ -norm of the error  $\|x - x_{k-1}\|_A$  (solid curve) and the upper bounds for the considered values of  $\mu_i$ ,  $i = 3, 8, 16, 50$  (dotted solid curves). The dots represent the values  $\theta_1^{(k)} - \lambda_1$ , i.e., the distances of the smallest Ritz values  $\theta_1^{(k)}$  to  $\lambda_1$ . The horizontal dotted lines correspond to the values of  $\lambda_1 - \mu_i$ ,  $i = 3, 8, 16$ .

The upper bounds in Figure 4.1 first overestimate, and then closely approximate  $\|x - x_{k-1}\|_A$  (starting from iteration 5). However, at some point, the upper bounds start to differ significantly from  $\|x - x_{k-1}\|_A$  and represent much worse approximations, except for  $\mu_{50}$ . We observe that for a given  $\mu_i$ ,  $i = 3, 8, 16$ , the upper bounds are delayed when the distance of  $\theta_1^{(k)}$  to  $\lambda_1$  becomes smaller than the distance of  $\mu_i$  to  $\lambda_1$ , i.e., when

$$(4.4) \quad \theta_1^{(k)} - \lambda_1 < \lambda_1 - \mu_i.$$

If (4.4) holds, then the smallest Ritz value  $\theta_1^{(k)}$  is a better approximation to  $\lambda_1$  than  $\mu_i$ . This moment is emphasized using vertical dashed lines that connect the value  $\theta_1^{(k)} - \lambda_1$  with  $\|x - x_{k-1}\|_A$  in the first iteration  $k$  such that (4.4) holds. Moreover, below a certain level, the upper bounds become almost independent of  $\mu_i$ ,  $i = 3, 8, 16$ , and coincide. The closer is  $\mu$  to  $\lambda_1$ , the later this phenomenon occurs.



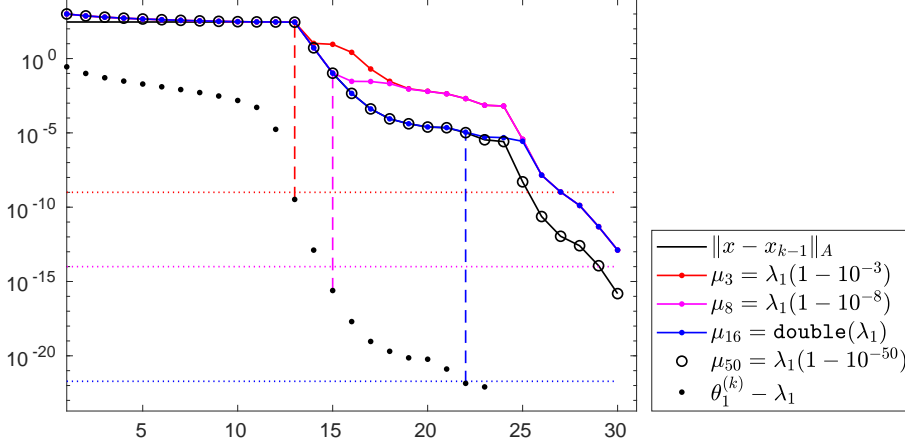


FIG. 4.1.  $\|x - x_{k-1}\|_A$ , upper bounds and the distance of  $\theta_1^{(k)}$  to the smallest eigenvalue  $\lambda_1$ , digits=128.

Depending on the validity of (4.4), we distinguish between *phase 1* and *phase 2* of convergence. If the inequality (4.4) does not hold, i.e., if  $\mu$  is a better approximation to  $\lambda_1$  than the smallest Ritz value, then we say we are in phase 1; see Figure 4.2. If (4.4) holds, then the smallest Ritz value is closer to  $\lambda_1$  than  $\mu$  and we are in phase 2; see Figure 4.3. Obviously, the beginning of phase 2 depends on the choice of  $\mu$  and on the convergence of the smallest Ritz value to the smallest eigenvalue. Note that for  $\mu = \mu_{50}$  we are always in phase 1 before we stop the iterations. In the following we would like to explain the phenomenon observed in Figure 4.1.

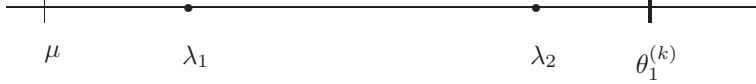


FIG. 4.2. Phase 1:  $\mu$  is a better approximation to  $\lambda_1$  than  $\theta_1^{(k)}$ .

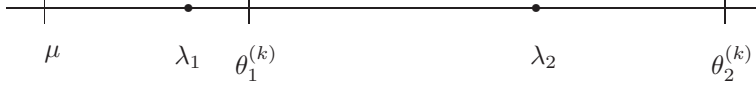


FIG. 4.3. Phase 2:  $\theta_1^{(k)}$  is a better approximation to  $\lambda_1$  than  $\mu$ .

**5. Analysis.** The upper bounds are computed from the modified tridiagonal matrices (2.5) discussed in Section 2.2, that differ only in one coefficient at the position  $(k+1, k+1)$ . Therefore, the first step of the analysis is to understand how the choice of  $\mu$  and the validity of the condition (4.4) influences the value of the modified coefficient

$$(5.1) \quad \alpha_{k+1}^{(\mu)} = \mu + \sum_{i=1}^k \eta_{i,k}^{(\mu)}, \quad \eta_{i,k}^{(\mu)} = \frac{(\beta_k s_{k,i}^{(k)})^2}{\theta_i^{(k)} - \mu};$$

see (2.8). We will compare its value to a modified coefficient for which phase 2 does not occur; see Figure 4.1 for  $\mu_{50}$ .

Based on that understanding we will then address further important questions. First, our aim is to explain the behaviour of the basic Gauss-Radau upper bound (3.8) in phase 2, in particular, its closeness to the rightmost upper bound in (3.5) that will be called *simple upper bound* in the following. Second, for practical reasons, without knowing  $\lambda_1$ , we would like to be able to detect phase 2, i.e., the first iteration  $k$  for which the inequality (4.4) starts to hold. Finally, we address the problem of how to improve the accuracy of the basic Gauss-Radau upper bound (3.8) in phase 2.

**5.1. The modified coefficient  $\alpha_{k+1}^{(\mu)}$ .** We first analyze the relation between two modified coefficients  $\alpha_{k+1}^{(\mu)}$  and  $\alpha_{k+1}^{(\lambda)}$  where  $0 < \mu < \lambda < \theta_1^{(k)}$ .

LEMMA 5.1. *Let  $0 < \mu < \lambda < \theta_1^{(k)}$ . Then*

$$(5.2) \quad \frac{\eta_{i,k}^{(\lambda)} - \eta_{i,k}^{(\mu)}}{\eta_{i,k}^{(\mu)}} = \frac{\lambda - \mu}{\theta_i^{(k)} - \lambda}$$

and

$$(5.3) \quad \alpha_{k+1}^{(\lambda)} - \alpha_{k+1}^{(\mu)} = \left( \frac{\lambda - \mu}{\theta_1^{(k)} - \mu} \right) \eta_{1,k}^{(\lambda)} + (\lambda - \mu) E_k^{(\lambda, \mu)}$$

where

$$(5.4) \quad E_k^{(\lambda, \mu)} \equiv 1 + \sum_{i=2}^k \frac{\eta_{i,k}^{(\lambda)}}{\theta_i^{(k)} - \mu}$$

satisfies  $E_k^{(\lambda, \mu)} = E_k^{(\mu, \lambda)}$ .

*Proof.* The relation (5.2) follows immediately from the definition of  $\eta_{i,k}^{(\mu)}$  and  $\eta_{i,k}^{(\lambda)}$ ,

$$\frac{\eta_{i,k}^{(\lambda)} - \eta_{i,k}^{(\mu)}}{\eta_{i,k}^{(\mu)}} = \frac{\frac{(\beta_k s_{k,i}^{(k)})^2}{\theta_i^{(k)} - \lambda} - \frac{(\beta_k s_{k,i}^{(k)})^2}{\theta_i^{(k)} - \mu}}{\frac{(\beta_k s_{k,i}^{(k)})^2}{\theta_i^{(k)} - \mu}} = \frac{\lambda - \mu}{\theta_i^{(k)} - \lambda}.$$

Note that  $0 < \eta_{i,k}^{(\mu)} < \eta_{i,k}^{(\lambda)}$ . The difference of the coefficients  $\alpha$ 's is

$$\begin{aligned} \alpha_{k+1}^{(\lambda)} - \alpha_{k+1}^{(\mu)} &= (\lambda - \mu) + \sum_{i=1}^k (\eta_{i,k}^{(\lambda)} - \eta_{i,k}^{(\mu)}) \\ &= (\lambda - \mu) + \sum_{i=1}^k \left( \frac{(\beta_k s_{k,i}^{(k)})^2}{\theta_i^{(k)} - \lambda} - \frac{(\beta_k s_{k,i}^{(k)})^2}{\theta_i^{(k)} - \mu} \right) \\ &= (\lambda - \mu) + (\lambda - \mu) \sum_{i=1}^k \frac{(\beta_k s_{k,i}^{(k)})^2}{(\theta_i^{(k)} - \lambda)(\theta_i^{(k)} - \mu)} \\ &= (\lambda - \mu) \frac{\eta_{1,k}^{(\lambda)}}{\theta_1^{(k)} - \mu} + (\lambda - \mu) + (\lambda - \mu) \sum_{i=2}^k \frac{\eta_{i,k}^{(\lambda)}}{\theta_i^{(k)} - \mu} \end{aligned}$$

which implies (5.3). Since,

$$\frac{\eta_{i,k}^{(\lambda)}}{\theta_i^{(k)} - \mu} = \frac{\eta_{i,k}^{(\mu)}}{\theta_i^{(k)} - \lambda},$$

it holds that  $E_k^{(\lambda,\mu)} = E_k^{(\mu,\lambda)}$ .  $\square$

Let us describe in more detail the situation we are interested in. Suppose that  $\lambda_1$  is well separated from  $\lambda_2$ , and that  $\mu$  is a tight underestimate to  $\lambda_1$  such that

$$(5.5) \quad \lambda_1 - \mu \ll \lambda_2 - \lambda_1.$$

We would like to compare  $\alpha_{k+1}^{(\lambda_1)}$  for which phase 2 does not occur with  $\alpha_{k+1}^{(\mu)}$  for which phase 2 occurs; see Figure 4.1. Using (5.2) and (5.5), we are able to compare the individual  $\eta$ -terms. In particular, for  $i > 1$  we obtain

$$\frac{\eta_{i,k}^{(\lambda_1)} - \eta_{i,k}^{(\mu)}}{\eta_{i,k}^{(\mu)}} < \frac{\lambda_1 - \mu}{\lambda_2 - \lambda_1} \ll 1,$$

i.e.,

$$\eta_{i,k}^{(\lambda_1)} \approx \eta_{i,k}^{(\mu)} \quad \text{for } i > 1.$$

Hence,  $\alpha_{k+1}^{(\mu)}$  can significantly differ from  $\alpha_{k+1}^{(\lambda_1)}$  only in the first term of the sum in (5.1) for which

$$(5.6) \quad \frac{\eta_{1,k}^{(\lambda_1)} - \eta_{1,k}^{(\mu)}}{\eta_{1,k}^{(\mu)}} = \frac{\lambda_1 - \mu}{\theta_1^{(k)} - \lambda_1}.$$

If  $\theta_1^{(k)}$  is a better approximation to  $\lambda_1$  than  $\mu$  in the sense of (4.4), see Figure 4.3, then (5.6) shows that  $\eta_{1,k}^{(\lambda_1)}$  can be much larger than  $\eta_{1,k}^{(\mu)}$ . As a consequence,  $\alpha_{k+1}^{(\lambda_1)}$  can differ significantly from  $\alpha_{k+1}^{(\mu)}$ . On the other hand, if  $\mu$  is chosen such that

$$\lambda_1 - \mu \ll \theta_1^{(k)} - \lambda_1,$$

for all  $k$  we are interested in, then phase 2 will not occur, and

$$\alpha_{k+1}^{(\mu)} \approx \alpha_{k+1}^{(\lambda_1)}.$$

In the following we discuss phase 1 and phase 2 in more detail.

**5.2. Phase 1.** In phase 1,

$$\lambda_1 - \mu < \theta_1^{(k)} - \lambda_1,$$

and, therefore, all components  $\eta_{i,k}^{(\mu)}$  (including  $\eta_{1,k}^{(\mu)}$ ) are not sensitive to small changes of  $\mu$ ; see (5.2). In other words, the coefficients  $\alpha_{k+1}^{(\mu)}$  are approximately the same for various choices of  $\mu$ .

Let us denote

$$h = \frac{\lambda_1 - \mu}{\theta_1^{(k)} - \lambda_1} < 1.$$

In fact, we can write  $\theta_1^{(k)} - \mu = \theta_1^{(k)} - \lambda_1 + \lambda_1 - \mu$  and use the Taylor expansion of  $1/(1+h)$ . It yields

$$\frac{1}{\theta_1^{(k)} - \mu} = \frac{1}{\theta_1^{(k)} - \lambda_1} \left( \frac{1}{h+1} \right) = \frac{1}{\theta_1^{(k)} - \lambda_1} [1 - h + h^2 - h^3 + \dots].$$

At the beginning of the iterations,  $\theta_1^{(k)} - \lambda_1$  is large compared to  $\lambda_1 - \mu$ ,  $h$  is small and the right-hand side of  $1/(\theta_1^{(k)} - \mu)$  is almost given by  $1/(\theta_1^{(k)} - \lambda_1)$ , independent of  $\mu$ . Moreover, the last components  $s_{k,i}^{(k)}$  squared are not very small and the first term of the sum of the  $\eta_{i,k}^{(\mu)}$  is the largest one.

**5.3. Phase 2.** First recall that for any  $0 < \mu < \lambda_1$  it holds that

$$(5.7) \quad \alpha_{k+1}^{(\mu)} < \alpha_{k+1}^{(\lambda_1)} \quad \text{and} \quad \eta_{1,k}^{(\mu)} < \eta_{1,k}^{(\lambda_1)}.$$

As before, suppose that  $\lambda_1$  is well separated from  $\lambda_2$  and that (5.5) holds. Phase 2 begins when  $\theta_1^{(k)}$  is a better approximation to  $\lambda_1$  than  $\mu$ , i.e., when (4.4) holds. Since  $\theta_1^{(k)}$  is a tight approximation to  $\lambda_1$  in phase 2, (2.3) and (4.4) imply that

$$(5.8) \quad \eta_{1,k}^{(\lambda_1)} \geq \lambda_2 - \theta_1^{(k)} = \lambda_2 - \lambda_1 + \lambda_1 - \theta_1^{(k)} > (\lambda_2 - \lambda_1) - (\lambda_1 - \mu).$$

Therefore, using (5.5),  $\eta_{1,k}^{(\lambda_1)}$  is bounded away from zero. On the other hand, (2.3) also implies that

$$\eta_{1,k}^{(\mu)} = \frac{\theta_1^{(k)} - \lambda_1}{\theta_1^{(k)} - \mu} \eta_{1,k}^{(\lambda_1)} \leq \frac{\theta_1^{(k)} - \lambda_1}{\theta_1^{(k)} - \mu} (\lambda_n - \lambda_1)$$

and as  $\theta_1^{(k)}$  converges to  $\lambda_1$ ,  $\eta_{1,k}^{(\mu)}$  goes to zero. Therefore,

$$\alpha_{k+1}^{(\mu)} \approx \mu + \sum_{i=2}^k \eta_{i,k}^{(\mu)},$$

and the sum on the right-hand side is almost independent of  $\mu$ . Note that having two values  $0 < \mu < \lambda < \lambda_1$  such that

$$(5.9) \quad \theta_1^{(k)} - \lambda_1 < \lambda_1 - \lambda \quad \text{and} \quad \lambda - \mu \ll \lambda_2 - \lambda_1,$$

then one can expect that

$$(5.10) \quad \alpha_{k+1}^{(\mu)} \approx \alpha_{k+1}^{(\lambda)}$$

because  $\eta_{1,k}^{(\mu)}$  and  $\eta_{1,k}^{(\lambda)}$  converge to zero and  $\eta_{i,k}^{(\mu)} \approx \eta_{i,k}^{(\lambda)}$  for  $i > 1$  due to

$$\frac{\eta_{i,k}^{(\lambda)} - \eta_{i,k}^{(\mu)}}{\eta_{i,k}^{(\mu)}} = \frac{\lambda - \mu}{\theta_i^{(k)} - \lambda} < \frac{\lambda - \mu}{\lambda_2 - \lambda_1} \ll 1,$$

where we have used (5.2) and the assumption (5.9). Therefore,  $\alpha_{k+1}^{(\mu)}$  is relatively insensitive to small changes of  $\mu$  and the same is true for the upper bound (3.8).

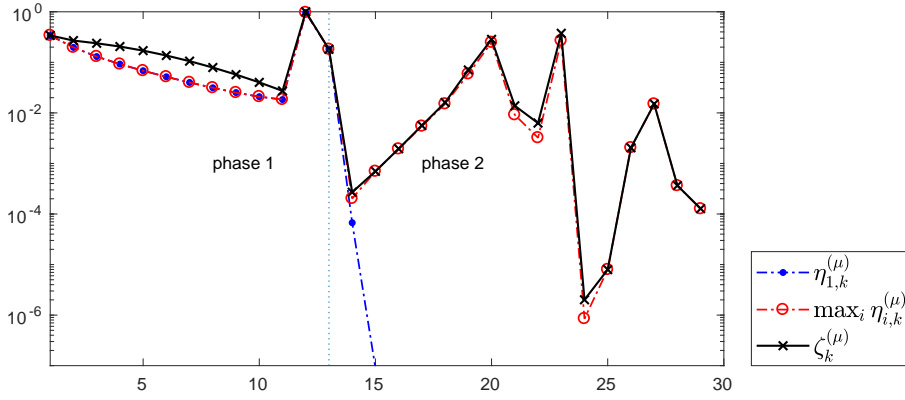


FIG. 5.1. First term  $\eta_{1,k}^{(\mu)}$ , maximum term  $\eta_{i,k}^{(\mu)}$ , and the sum  $\zeta_k^{(\mu)}$  for  $\mu = \mu_3$ .

Let us demonstrate the theoretical results numerically using our model problem. To compute the following results, we, again, use Matlab's vpa arithmetic with 128 digits.

We first consider  $\mu = \mu_3 = (1 - 10^{-3})\lambda_1$  for which we have  $\lambda_1 - \mu = 10^{-9}$ . The switch from phase 1 to phase 2 occurs at iteration 13. Figure 5.1 displays the first term  $\eta_{1,k}^{(\mu)}$  and the maximum term  $\eta_{i,k}^{(\mu)}$  as well as the sum  $\zeta_k^{(\mu)}$  defined by (2.9), see Lemma 2.1, as a function of the iteration number  $k$ . In phase 1 the first term  $\eta_{1,k}^{(\mu)}$  is the largest one. As predicted, after the start of phase 2, the first term is decreasing quite fast.

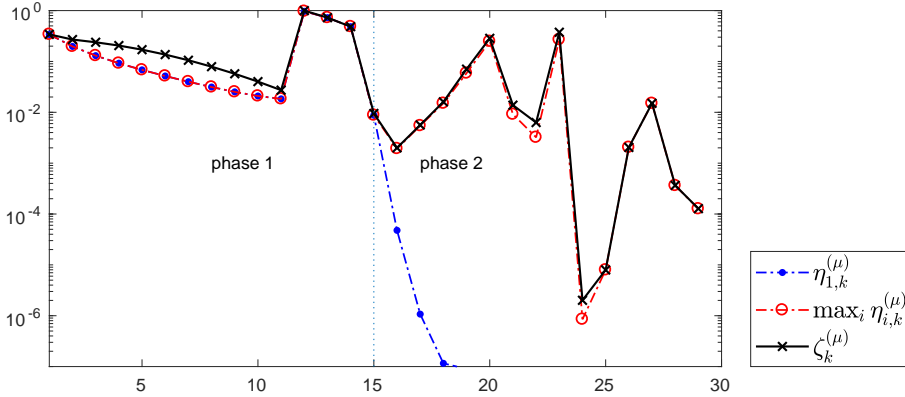


FIG. 5.2. First term  $\eta_{1,k}^{(\mu)}$ , maximum term  $\eta_{i,k}^{(\mu)}$ , and the sum  $\zeta_k^{(\mu)}$  for  $\mu = \mu_8$ .

Let us now use  $\mu = \mu_8 = (1 - 10^{-8})\lambda_1$  for which we have  $\lambda_1 - \mu = 10^{-14}$ . The switch from phase 1 to phase 2 occurs at iteration 15; see Figure 5.2. The conclusions are the same as for  $\mu_3$ .

The behavior of the first term is completely different for  $\mu = (1 - 10^{-50})\lambda_1$  which almost corresponds to using the exact smallest eigenvalue  $\lambda_1$ ; see Figure 4.3. The maximum term of the sum is then almost always the first one; see Figure 5.3. Remember that, for this value of  $\mu$ , we are always in phase 1.

Finally, in Figure 5.4 we present a comparison of the sums  $\zeta_k^{(\mu)}$  for  $\mu_3$ ,  $\mu_8$ , and

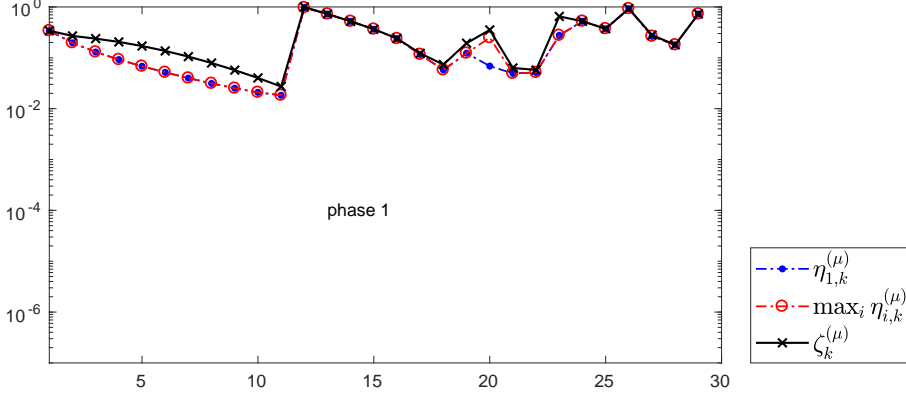


FIG. 5.3. First term  $\eta_{1,k}^{(\mu)}$ , maximum term  $\eta_{i,k}^{(\mu)}$ , and the sum  $\zeta_k^{(\mu)}$  for  $\mu = \mu_{50}$ .

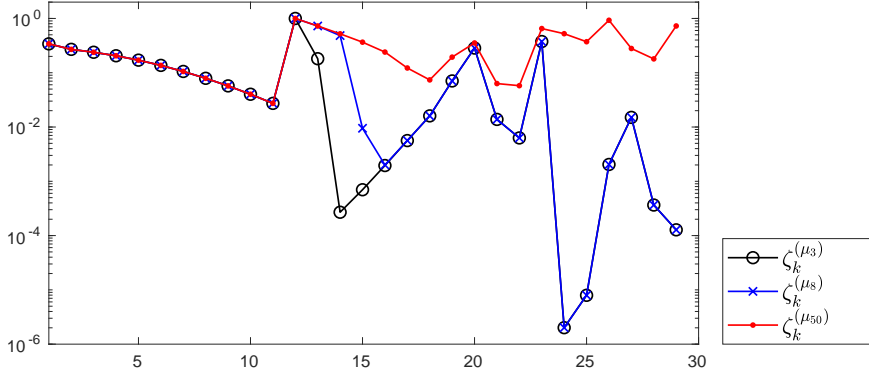


FIG. 5.4. Comparison of the sums  $\zeta_k^{(\mu_3)}$ ,  $\zeta_k^{(\mu_8)}$ , and  $\zeta_k^{(\mu_{50})}$ .

$\mu_{50}$ . We observe that from the beginning up to iteration 12, all sums visually coincide. Starting from iteration 13 we enter phase 2 for  $\mu = \mu_3$  and the sum  $\zeta_k^{(\mu_3)}$  starts to differ significantly from the other sums, in particular from the “reference” term  $\zeta_k^{(\mu_{50})}$ . Similarly, for  $k = 15$  we enter phase 2 for  $\mu = \mu_8$  and  $\zeta_k^{(\mu_8)}$  and  $\zeta_k^{(\mu_{50})}$  start to differ. We can also observe that  $\zeta_k^{(\mu_3)}$  and  $\zeta_k^{(\mu_8)}$  significantly differ only in iterations 13, 14, and 15, i.e., when we are in phase 2 for  $\mu = \mu_3$  but in phase 1 for  $\mu = \mu_8$ . In all other iterations,  $\zeta_k^{(\mu_3)}$  and  $\zeta_k^{(\mu_8)}$  visually coincide.

**5.4. The coefficient  $\alpha_{k+1}$ .** The coefficient  $\alpha_{k+1}$  can also be written as

$$\alpha_{k+1} = \alpha_{k+1}^{(\mu)} \quad \text{for} \quad \mu = \theta_1^{(k+1)},$$

and the results of Lemma 2.1 and Lemma 5.1 are still valid, even though, in practice,  $\mu$  must be smaller than  $\lambda_1$ . Using (5.3) we can express the differences between the coefficients, it holds that

$$(5.11) \quad \alpha_{k+1} - \alpha_{k+1}^{(\lambda_1)} = \eta_{1,k}^{(\lambda_1)} \frac{\theta_1^{(k+1)} - \lambda_1}{\theta_1^{(k)} - \theta_1^{(k+1)}} + \left( \theta_1^{(k+1)} - \lambda_1 \right) E_k^{(\theta_1^{(k+1)}, \lambda_1)}.$$

If the smallest Ritz value  $\theta_1^{(k+1)}$  is close to  $\lambda_1$ , then the second term of the right-hand side in (5.11) will be negligible in comparison to the first one, since

$$E_k^{(\theta_1^{(k+1)}, \lambda_1)} = \mathcal{O}(1),$$

see (5.4), and since  $\eta_{1,k}^{(\lambda_1)}$  is bounded away from zero; see (5.8). Therefore, one can expect that

$$(5.12) \quad \alpha_{k+1} - \alpha_{k+1}^{(\lambda_1)} \approx \eta_{1,k}^{(\lambda_1)} \frac{\theta_1^{(k+1)} - \lambda_1}{\theta_1^{(k)} - \theta_1^{(k+1)}}.$$

The size of the term on the right-hand side is related to the speed of convergence of the smallest Ritz value  $\theta_1^{(k)}$  to  $\lambda_1$ . Denoting

$$\frac{\theta_1^{(k+1)} - \lambda_1}{\theta_1^{(k)} - \lambda_1} = \rho_k < 1,$$

we obtain

$$\frac{\theta_1^{(k+1)} - \lambda_1}{\theta_1^{(k)} - \theta_1^{(k+1)}} = \frac{\frac{\theta_1^{(k+1)} - \lambda_1}{\theta_1^{(k)} - \lambda_1}}{1 - \frac{\theta_1^{(k+1)} - \lambda_1}{\theta_1^{(k)} - \lambda_1}} = \frac{\rho_k}{1 - \rho_k}.$$

For example, if the convergence of  $\theta_1^{(k)}$  to  $\lambda_1$  is superlinear, i.e., if  $\rho_k \rightarrow 0$ , then  $\alpha_{k+1}$  tends to be very close to  $\alpha_{k+1}^{(\lambda_1)}$ .

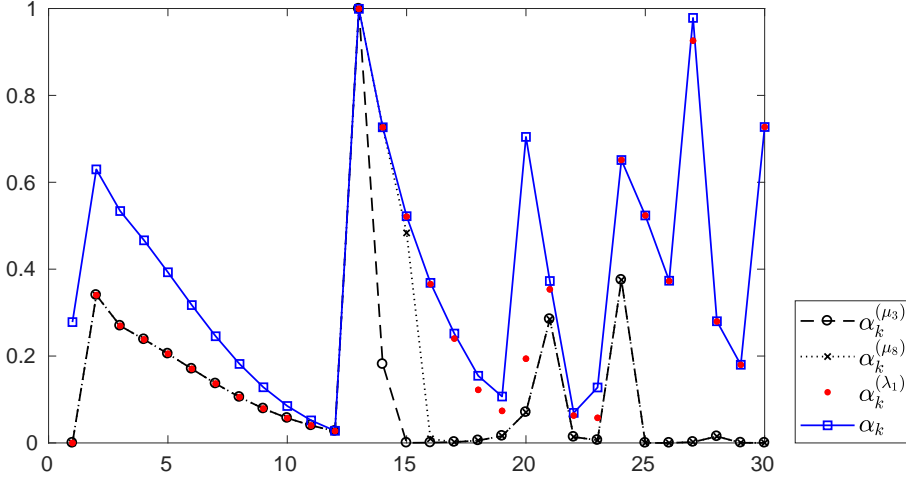


FIG. 5.5.  $\alpha_k^{(\mu_3)}$ ,  $\alpha_k^{(\mu_8)}$ ,  $\alpha_k^{(\lambda_1)}$ , and  $\alpha_k$ .

In Figure 5.5 we plot the coefficients  $\alpha_k^{(\mu_3)}$ ,  $\alpha_k^{(\mu_8)}$ ,  $\alpha_k^{(\lambda_1)}$  and  $\alpha_k$ , so that we can compare the observed behaviour with the predicted one. Phase 2 starts for  $\mu_3$  at iteration 13, and for  $\mu_8$  at iteration 15; see also Figure 4.1. For  $k \leq 13$  we observe that

$$\alpha_k^{(\mu_3)} \approx \alpha_k^{(\mu_8)} \approx \alpha_k^{(\lambda_1)}$$

as explained in Section 5.2 and  $\alpha_k$  is larger. For  $k \geq 16$ , the first terms  $\eta_{1,k-1}^{(\mu_3)}$  and  $\eta_{1,k-1}^{(\mu_8)}$  are close to zero, and, as explained in Section 5.3,

$$\alpha_k^{(\mu_3)} \approx \alpha_k^{(\mu_8)}.$$

For  $k = 14$  and  $k = 15$ ,  $\alpha_k^{(\mu_3)}$  and  $\alpha_k^{(\mu_8)}$  can differ significantly because  $\alpha_k^{(\mu_3)}$  is already in phase 2 while  $\alpha_k^{(\mu_8)}$  is still in phase 1.

We can also observe that  $\alpha_k$  can be very close to  $\alpha_k^{(\lambda_1)}$  when the smallest Ritz value  $\theta_1^{(k)}$  is a tight approximation to  $\lambda_1$ , i.e., in later iterations. We know that the closeness of  $\alpha_k$  to  $\alpha_k^{(\lambda_1)}$  depends on the speed of convergence of the smallest Ritz value to  $\lambda_1$ ; see (5.12) and the corresponding discussion.

**6. The Gauss-Radau bound in phase 2.** Our aim in this section is to investigate the relation between the basic Gauss-Radau upper bound (3.8) and the simple upper bound; see (3.5). Recall the notation

$$\phi_k = \frac{\|r_k\|^2}{\|p_k\|^2};$$

see (3.6). In particular, we would like to explain why the two bounds almost coincide in phase 2. Note that using (3.4) we obtain

$$(6.1) \quad \alpha_{k+1}^{(\mu)} = \left( \gamma_k^{(\mu)} \right)^{-1} + \frac{\delta_k}{\gamma_{k-1}}$$

and from (2.8) it follows

$$\alpha_{k+1}^{(\mu)} = \mu + \beta_k^2 e_k^T (T_k - \mu I)^{-1} e_k, \quad \beta_k^2 = \frac{1}{\gamma_{k-1}} \frac{\delta_k}{\gamma_{k-1}}.$$

Therefore,

$$(6.2) \quad \left( \gamma_k^{(\mu)} \right)^{-1} = \mu + \beta_k^2 \left( e_k^T (T_k - \mu I)^{-1} e_k - \gamma_{k-1} \right).$$

In the following lemma we find another expression for  $e_k^T (T_k - \mu I)^{-1} e_k$ .

LEMMA 6.1. *Let  $0 < \mu < \theta_1^{(k)}$ . Then it holds that*

$$(6.3) \quad e_k^T (T_k - \mu I)^{-1} e_k = \gamma_{k-1} + \mu \frac{\gamma_{k-1}^2}{\phi_{k-1}} + \sum_{i=1}^k \left( \frac{\mu}{\theta_i^{(k)}} \right)^2 \frac{\left( s_{k,i}^{(k)} \right)^2}{\theta_i^{(k)} - \mu}.$$

*Proof.* Since  $\|\mu T_k^{-1}\| < 1$ , we obtain using a Neumann series

$$(T_k - \mu I)^{-1} = (I - \mu T_k^{-1})^{-1} T_k^{-1} = \left( \sum_{j=0}^{\infty} \mu^j T_k^{-j} \right) T_k^{-1}$$

so that

$$e_k^T (T_k - \mu I)^{-1} e_k = e_k^T T_k^{-1} e_k + \mu e_k^T T_k^{-2} e_k + \sum_{j=2}^{\infty} \mu^j e_k^T T_k^{-(j+1)} e_k.$$



We now express the terms on the right-hand side using the CG coefficients and the quantities from the spectral factorization of  $T_k$ . Using  $T_k = L_k D_k L_k^T$  we obtain  $e_k^T T_k^{-1} e_k = \gamma_{k-1}$ . After some algebraic manipulation, see, e.g., [15, p. 1369] we get

$$T_k^{-1} e_k = \gamma_{k-1} \|r_{k-1}\| \begin{bmatrix} \frac{(-1)^{k-1}}{\|r_0\|} \\ \vdots \\ \frac{1}{\|r_{k-1}\|} \end{bmatrix}$$

so that

$$e_k^T T_k^{-2} e_k = e_k^T T_k^{-1} T_k^{-1} e_k = \gamma_{k-1}^2 \sum_{i=0}^{k-1} \frac{\|r_{k-1}\|^2}{\|r_i\|^2} = \gamma_{k-1}^2 \frac{\|p_{k-1}\|^2}{\|r_{k-1}\|^2} = \frac{\gamma_{k-1}^2}{\phi_{k-1}}.$$

Finally,

$$e_k^T \left( \sum_{j=2}^{\infty} \mu^j T_k^{-(j+1)} \right) e_k = e_k^T S_k \left( \sum_{j=2}^{\infty} \mu^j \Theta_k^{-(j+1)} \right) S_k^T e_k$$

where the diagonal entries of the diagonal matrix

$$\sum_{j=2}^{\infty} \mu^j \Theta_k^{-(j+1)}$$

have the form

$$\frac{1}{\theta_i^{(k)}} \left( \frac{\mu}{\theta_i^{(k)}} \right)^2 \sum_{j=0}^{\infty} \left( \frac{\mu}{\theta_i^{(k)}} \right)^j = \frac{1}{\theta_i^{(k)}} \left( \frac{\mu}{\theta_i^{(k)}} \right)^2 \frac{1}{1 - \frac{\mu}{\theta_i^{(k)}}} = \left( \frac{\mu}{\theta_i^{(k)}} \right)^2 \frac{1}{\theta_i^{(k)} - \mu}.$$

Hence,

$$e_k^T \left( \sum_{j=2}^{\infty} \mu^j T_k^{-(j+1)} \right) e_k = \sum_{i=1}^k \left( \frac{\mu}{\theta_i^{(k)}} \right)^2 \frac{(s_{k,i}^{(k)})^2}{\theta_i^{(k)} - \mu}.$$

□

Based on the previous lemma we can now express the coefficient  $\gamma_k^{(\mu)}$ .

**THEOREM 6.2.** *Let  $0 < \mu < \theta_1^{(k)}$ . Then it holds that*

$$(6.4) \quad \left( \gamma_k^{(\mu)} \right)^{-1} = \frac{\mu}{\phi_k} + \sum_{i=1}^k \left( \frac{\mu}{\theta_i^{(k)}} \right)^2 \eta_{i,k}^{(\mu)}.$$

*Proof.* We start with (6.2). Using the previous lemma

$$\begin{aligned} \left( \gamma_k^{(\mu)} \right)^{-1} &= \mu + \mu \beta_k^2 \gamma_{k-1}^2 \phi_{k-1}^{-1} + \beta_k^2 e_k^T \left( \sum_{j=2}^{\infty} \mu^j T_k^{-(j+1)} \right) e_k \\ &= \mu (1 + \delta_k \phi_{k-1}^{-1}) + \beta_k^2 \sum_{i=1}^k \left( \frac{\mu}{\theta_i^{(k)}} \right)^2 \frac{(s_{k,i}^{(k)})^2}{\theta_i^{(k)} - \mu} \\ &= \mu \phi_k^{-1} + \sum_{i=1}^k \left( \frac{\mu}{\theta_i^{(k)}} \right)^2 \frac{(\beta_k s_{k,i}^{(k)})^2}{\theta_i^{(k)} - \mu}, \end{aligned}$$

where we have used relation (3.6).  $\square$

Obviously, using (6.4), the basic Gauss-Radau upper bound (3.8) and the simple upper bound in (3.5) are close to each other if and only if

$$(6.5) \quad \sum_{i=1}^k \left( \frac{\mu}{\theta_i^{(k)}} \right)^2 \eta_{i,k}^{(\mu)} \ll \frac{\mu}{\phi_k},$$

which can also be written as

$$(6.6) \quad \left( \frac{\mu}{\theta_1^{(k)}} \right)^2 \frac{\eta_{1,k}^{(\mu)}}{\mu} + \sum_{i=2}^k \left( \frac{\beta_k s_{k,i}^{(k)}}{\theta_i^{(k)}} \right)^2 \frac{\mu}{\theta_i^{(k)} - \mu} \ll \phi_k^{-1}.$$

Assuming as before that  $\lambda_1$  is well separated from  $\lambda_2$ , and that  $\mu$  is a tight underestimate to  $\lambda_1$  in the sense of (5.5), the sum of terms on the left-hand side of (6.6) can be replaced by its tight upper bound

$$(6.7) \quad \left( \frac{\lambda_1}{\theta_1^{(k)}} \right)^2 \frac{\eta_{1,k}^{(\mu)}}{\mu} + \sum_{i=2}^k \left( \frac{\beta_k s_{k,i}^{(k)}}{\theta_i^{(k)}} \right)^2 \frac{\lambda_1}{\theta_i^{(k)} - \lambda_1}$$

which simplifies the explanation of the dependence of the sum in (6.6) on  $\mu$ .

The second term in (6.7) is independent of  $\mu$  and its size depends only on the behaviour of the underlying Lanczos process. Here

$$(6.8) \quad \left( \frac{\beta_k s_{k,i}^{(k)}}{\theta_i^{(k)}} \right)^2 = \frac{\|A(V_k s_{:,i}^{(k)}) - \theta_i^{(k)}(V_k s_{:,i}^{(k)})\|^2}{(\theta_i^{(k)})^2}$$

can be seen as the relative accuracy to which the  $i$ th Ritz value approximates an eigenvalue, and the size of the term

$$(6.9) \quad \frac{\lambda_1}{\theta_i^{(k)} - \lambda_1}, \quad i \geq 2,$$

depends on the position of  $\theta_i^{(k)}$  relatively to the smallest eigenvalue. In particular, one can expect that the term (6.9) can be of size  $\mathcal{O}(1)$  if  $\theta_i^{(k)}$  approximates smallest eigenvalues, and it is small if  $\theta_i^{(k)}$  approximates largest eigenvalues.

Using the previous simplifications and assuming phase 2, the basic Gauss-Radau upper bound (3.8) and the rightmost upper bound in (3.5) are close to each other if and only if

$$(6.10) \quad \frac{\eta_{1,k}^{(\mu)}}{\mu} + \sum_{i=2}^k \left( \frac{\beta_k s_{k,i}^{(k)}}{\theta_i^{(k)}} \right)^2 \frac{\lambda_1}{\theta_i^{(k)} - \lambda_1} \ll \phi_k^{-1}.$$

From Section 5.3 we know that  $\eta_{1,k}^{(\mu)}$  goes to zero in phase 2. Hence, if

$$(6.11) \quad \eta_{1,k}^{(\mu)} < \mu,$$

which will happen for  $k$  sufficiently large, then the first term in (6.10) is smaller than the term on the right-hand side.

As already mentioned, the sum of positive terms in (6.10) depends only on approximation properties of the underlying Lanczos process, that are not easy to predict in general. Inspired by our model problem described in Section 4, we can just give an intuitive explanation why the sum could be small in phase 2.

Phase 2 occurs in later CG iterations and it is related to the convergence of the smallest Ritz value to the smallest eigenvalue. If the smallest eigenvalue is well approximated by the smallest Ritz value (to a high relative accuracy), then one can expect that many eigenvalues of  $A$  are relatively well approximated by Ritz values. If the eigenvalue  $\lambda_j$  of  $A$  is well separated from the other eigenvalues and if it is well approximated by a Ritz value, then the corresponding term (6.8) measuring the relative accuracy to which  $\lambda_j$  is approximated, is going to be small.

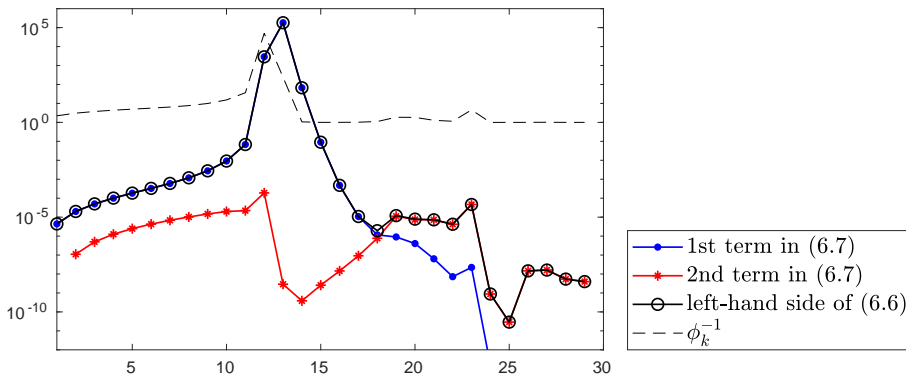


FIG. 6.1. Sizes of terms in (6.7) and (6.6).

In particular, in our model problem, the smallest eigenvalues are well separated from each other, and in phase 2 they are well approximated by Ritz values. Therefore, the corresponding terms (6.8) are small. Hence, the Ritz values that did not converge yet in phase 2, are going to approximate eigenvalues in clusters which do not correspond to smallest eigenvalues, i.e., for which the terms (6.9) are small; see also Figure 5.2 and Figure 5.1. In our model problem, the sum of positive terms in (6.10) is small in phase 2 because either (6.8) or (6.9) are small. Therefore, one can expect that the validity of (6.10) will mainly depend on the size of the first term in (6.10); see Figure 6.1.

The size of the sum of positive terms in (6.10) obviously depends on the clustering and the distribution of the eigenvalues, and we cannot guarantee in general that it will be small in phase 2. For example, it need not be small if the smallest eigenvalues of  $A$  are clustered.

**7. Detection of phase 2.** For our model problem it is not hard to detect phase 2 from the coefficients that are available during the computations. We first observe, see Figure 6.1, that the coefficients

$$(7.1) \quad \gamma_k^{(\mu)} \quad \text{and} \quad \frac{\phi_k}{\mu},$$

and the corresponding bounds (3.8) and (3.5) visually coincide from the beginning up to some iteration  $\ell_1$ . From iteration  $\ell_1 + 1$ , the Gauss-Radau upper bound (3.8) starts to be a much better approximation to the squared  $A$ -norm of the error than the simple upper bound (3.5). When phase 2 occurs, the Gauss-Radau upper bound

(3.8) loses its accuracy and, starting from iteration  $\ell_2$  (approximately when (6.11) holds), it will again visually coincide with the simple upper bound (3.5). We observe that phase 2 occurs at some iteration  $k$  where the two coefficients (7.1) significantly differ, i.e., for  $\ell_1 < k < \ell_2$ . To measure the agreement between the coefficients (7.1), we can use the easily computable relative distance

$$(7.2) \quad \frac{\frac{\phi_k}{\mu} - \gamma_k^{(\mu)}}{\gamma_k^{(\mu)}} = \phi_k \left[ \left( \frac{\mu}{\theta_1^{(k)}} \right)^2 \frac{\eta_{1,k}^{(\mu)}}{\mu} + \sum_{i=2}^k \left( \frac{\beta_k s_{k,i}^{(k)}}{\theta_i^{(k)}} \right)^2 \frac{\mu}{\theta_i^{(k)} - \mu} \right].$$

We will consider this relative distance to be small, if it is smaller than 0.5.

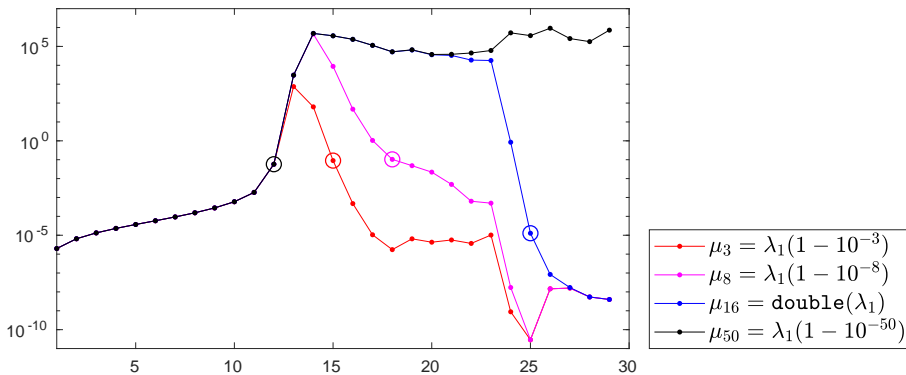


FIG. 7.1. The behaviour of the relative distance in (7.2) for various values of  $\mu$ .

The behavior of the term in (7.2) for various values of  $\mu$  is shown in Figure 7.1. The index  $\ell_1 = 12$  is the same for all considered values of  $\mu$ . For  $\mu_3$  we get  $\ell_2 = 15$  (red circle), for  $\mu_8$  we get  $\ell_2 = 18$  (magenta circle), for  $\mu_{16}$   $\ell_2 = 25$  (blue circle), and finally, for  $\mu_{50}$  there is no index  $\ell_2$ .

As explained in the previous section, in more complicated cases we cannot guarantee in general a similar behaviour of the relative distance (7.2) as in our model problem. For example, in practical problems we sometimes observe staircase behaviour of the  $A$ -norm of the error, when few iterations of stagnation are followed by few iterations of rapid convergence. In such cases, the quantity (7.2) can oscillate several times and it is much more difficult to use it for detecting phase 2. In general we can only say that when the smallest Ritz value is close enough to the smallest eigenvalue, the basic Gauss-Radau upper bound (3.8) can lose its accuracy even if  $\mu$  is close to  $\lambda_1$ , and it usually coincides with the simple upper bound (3.5). The formulas (6.4) and (7.2) can be helpful in understanding this behaviour.

**8. Improving the accuracy.** For integers  $\ell \geq k \geq 0$ , let us denote

$$\Delta_k = \gamma_k \|r_k\|^2, \quad \Delta_{k:\ell} = \sum_{j=k}^{\ell} \Delta_j, \quad \text{and} \quad \Delta_{k:k-1} = 0.$$

As described in [16], the accuracy of lower and upper bounds can be improved using

$$(8.1) \quad \varepsilon_k = \Delta_{k:\ell-1} + \varepsilon_{\ell},$$

where  $\varepsilon_j \equiv \|x - x_j\|_A^2$ ; see also (3.7). An improved bound at iteration  $k$  is obtained such that the last term in (8.1) is replaced by the basic lower or upper bounds on  $\varepsilon_{\ell}$ .

---

**Algorithm 3** CG with the improved Gauss-Radau upper bound
 

---

```

1: input  $A, b, x_0, \mu, \tau$ 
2:  $r_0 = b - Ax_0, p_0 = r_0$ 
3:  $k = 0, \gamma_0^{(\mu)} = \frac{1}{\mu}$ 
4: for  $\ell = 0, \dots, \mathbf{do}$ 
5:   cgiter( $\ell$ )
6:   while  $\ell \geq k$  and (8.4) do
7:     accept  $\Omega_{k:\ell}^{(\mu)}$ 
8:      $k = k + 1$ 
9:   end while
10:   $\gamma_{\ell+1}^{(\mu)} = \frac{\gamma_\ell^{(\mu)} - \gamma_\ell}{\mu(\gamma_\ell^{(\mu)} - \gamma_\ell) + \delta_{\ell+1}}$ 
11: end for

```

---

In particular, the improved Gauss-Radau upper bound can be defined as

$$(8.2) \quad \Omega_{k:\ell}^{(\mu)} = \Delta_{k:\ell-1} + \gamma_\ell^{(\mu)} \|r_\ell\|^2,$$

and the improved Gauss lower bound is given by  $\Delta_{k:\ell}$ .

To improve the accuracy of the Gauss-Radau upper bound, we would like to choose  $\ell$  such that the relative error of the improved Gauss-Radau upper bound is small enough, i.e.,

$$(8.3) \quad \frac{\Omega_{k:\ell}^{(\mu)} - \varepsilon_k}{\varepsilon_k} \leq \tau$$

where  $\tau$  is a prescribed tolerance, say,  $\tau = 0.25$ . Since

$$\frac{\Omega_{k:\ell}^{(\mu)} - \varepsilon_k}{\varepsilon_k} < \frac{\Omega_{k:\ell}^{(\mu)} - \Delta_{k:\ell}}{\Delta_{k:\ell}} = \frac{\|r_\ell\|^2 (\gamma_\ell^{(\mu)} - \gamma_\ell)}{\Delta_{k:\ell}},$$

we can require  $\ell \geq k$  to be the smallest integer such that

$$(8.4) \quad \frac{\|r_\ell\|^2 (\gamma_\ell^{(\mu)} - \gamma_\ell)}{\Delta_{k:\ell}} \leq \tau.$$

If (8.4) holds, then also (8.3) holds. The just described adaptive strategy for obtaining  $\ell$  giving a sufficiently accurate upper bound is summarized in Algorithm 3.

Note that

$$\frac{\Omega_{k:\ell}^{(\mu)} - \varepsilon_k}{\varepsilon_k} + \frac{\varepsilon_k - \Delta_{k:\ell}}{\varepsilon_k} < \frac{\Omega_{k:\ell}^{(\mu)} - \Delta_{k:\ell}}{\Delta_{k:\ell}},$$

i.e., if (8.4) holds, then  $\tau$  represents also an upper bound on the sum of relative errors of the improved lower and upper bounds. In other words, if  $\ell$  is such that (8.4) is satisfied, then both the improved Gauss-Radau upper bound as well as the improved Gauss lower bound are sufficiently accurate. Note that the index  $\ell$ , determined by Algorithm 3 that focuses on improving the accuracy of the Gauss-Radau upper bound, usually represents an overestimate of the optimal index  $\ell$  for the improved Gauss lower bound. For an adaptive heuristic strategy focused on improving the accuracy of the Gauss lower bound, see [16].

In the previous sections we have seen that the basic Gauss-Radau upper bound is delayed, in particular in phase 2. The delay of the basic Gauss-Radau upper bound can be defined as the smallest nonnegative integer  $j$  such that

$$(8.5) \quad \gamma_{k+j+1}^{(\mu)} \|r_{k+j+1}\|^2 < \varepsilon_k.$$

Having sufficiently accurate lower and upper bounds (e.g., if (8.4) is satisfied), we can approximately determine the delay of the basic Gauss-Radau upper bound as the smallest  $i$  satisfying (8.5) where  $\varepsilon_k$  in (8.5) is replaced by its tight lower bound  $\Lambda_{k,\ell}$ .

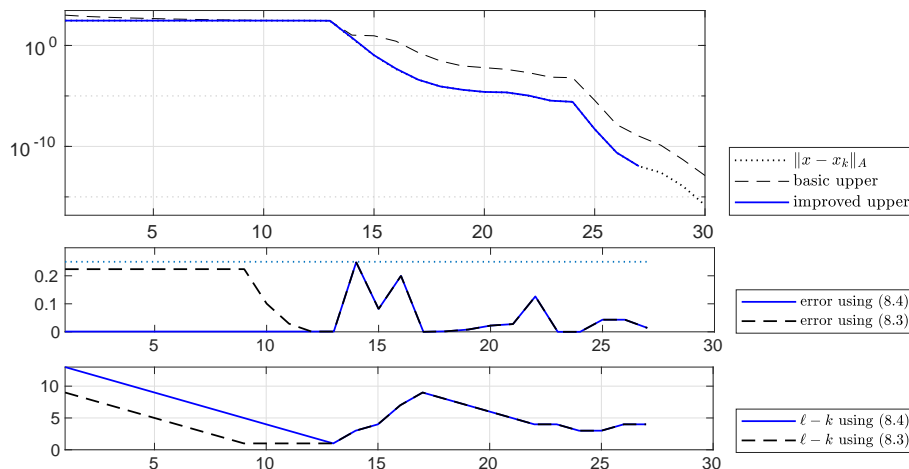


FIG. 8.1. Model problem and  $\mu_3 = \lambda_1(1 - 10^{-3})$ .

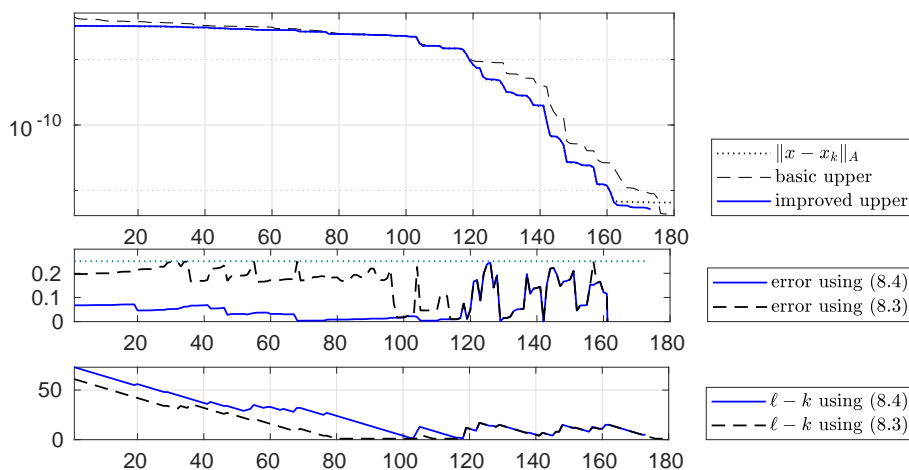


FIG. 8.2. Matrix `bcsstk01` and  $\mu_4 = \lambda_1(1 - 10^{-4})$ .

The strategy for improving the accuracy of the Gauss-Radau upper bound implemented in Algorithm 3 is demonstrated in Figure 8.1 and Figure 8.2. In Figure 8.1 we consider our model problem described in Section 4 and use Matlab's `vpa` arithmetic with 128 digits. In Figure 8.2 we consider the matrix `bcsstk01` of order 48 from the SuiteSparse Matrix collection and the unit norm right-hand side  $b$  that has

equal components in the eigenvector basis, choose  $\mu_4 = \lambda_1(1 - 10^{-4})$ , and run the experiment in the standard double precision arithmetic using MATLAB R2019b.

In the top parts of figures we plot the  $A$ -norm of the error (dotted), the square root of the basic Gauss-Radau upper bound (3.8) (dashed), and the square root of the improved Gauss-Radau upper bound (8.2) with  $\ell$  satisfying (8.4). We can see that the improved upper bound is visually the same as the  $A$ -norm of the error.

In the middle parts we plot the relative error

$$(8.6) \quad \frac{\Omega_{k:\ell}^{(\mu)} - \varepsilon_k}{\varepsilon_k}$$

(solid) together with the prescribed tolerance  $\tau = 0.25$  (dotted) where  $\ell$  was chosen using (8.4). For comparison we also plot the relative relative error (8.6) with the “ideal” value of  $\ell$ , i.e., with the smallest integer  $\ell \geq k$  such that (8.3) is satisfied. Note that the ideal value of  $\ell$  was determined using the quantities  $\varepsilon_k$  that are not available in practical computations.

Finally, in the bottom parts of Figure 8.1 and Figure 8.2 we plot the difference  $\ell - k$  at the individual iterations  $k$ , where  $\ell$  was determined using (8.4) (solid) or using (8.3) (dashed). We observe that in later iterations, the values of  $\ell$  satisfying the criterion (8.4) are almost ideal (optimal).

**9. Conclusions.** In this paper we discussed and analyzed the behaviour of the Gauss-Radau upper bound on the  $A$ -norm of the error in CG. In particular, we concentrated on the phenomenon observed during computations showing that, in later CG iterations, the upper bound loses its accuracy, it is almost independent of  $\mu$ , and visually coincides with the simple upper bound. We explained that this phenomenon is closely related to the convergence of the smallest Ritz value to the smallest eigenvalue of  $A$ . It occurs when the smallest Ritz value is a better approximation to the smallest eigenvalue than the prescribed underestimate  $\mu$ . We developed formulas that can be helpful in understanding this behavior, and suggested an adaptive strategy of how to improve the accuracy of the Gauss-Radau upper bound. Note that the loss of accuracy of the Gauss-Radau upper bound is not directly linked to rounding errors in computations of the bound, but it is related to the finite precision behaviour of the underlying Lanczos process. In more detail, the phenomenon can occur when solving linear systems with clustered eigenvalues. However, the results of finite precision CG computations can be seen (up to some small inaccuracies) as the results of the exact CG algorithm applied to a larger system with the system matrix having clustered eigenvalues. Therefore, one can expect that the discussed phenomenon can occur in practical computations not only when  $A$  has clustered eigenvalues, but also whenever orthogonality is lost in the CG algorithm.

#### REFERENCES

- [1] G. Dahlquist, S. C. Eisenstat, and G. H. Golub. Bounds for the error of linear systems of equations using the theory of moments. *J. Math. Anal. Appl.*, 37:151–166, 1972.
- [2] G. Dahlquist, G. H. Golub, and S. G. Nash. Bounds for the error in linear systems. In *Semi-infinite Programming (Proc. Workshop, Bad Honnef, 1978)*, volume 15 of *Lecture Notes in Control and Information Sci.*, pages 154–172. Springer, Berlin, 1979.
- [3] J. W. Demmel. *Applied Numerical Linear Algebra*. Society for Industrial and Applied Mathematics (SIAM), Philadelphia, PA, 1997.
- [4] G. H. Golub. Some modified matrix eigenvalue problems. *SIAM Rev.*, 15:318–334, 1973.

- [5] G. H. Golub and G. Meurant. Matrices, moments and quadrature. In *Numerical Analysis 1993 (Dundee, 1993)*, volume 303 of *Pitman Res. Notes Math. Ser.*, pages 105–156. Longman Sci. Tech., Harlow, 1994.
- [6] G. H. Golub and G. Meurant. Matrices, moments and quadrature. II. How to compute the norm of the error in iterative methods. *BIT*, 37(3):687–705, 1997.
- [7] G. H. Golub and Z. Strakoš. Estimates in quadratic formulas. *Numer. Algorithms*, 8(2-4):241–268, 1994.
- [8] W. B. Gragg and W. J. Harrod. The numerically stable reconstruction of Jacobi matrices from spectral data. *Numer. Math.*, 44(3):317–335, 1984.
- [9] A. Greenbaum. Behavior of slightly perturbed Lanczos and conjugate-gradient recurrences. *Linear Algebra Appl.*, 113:7–63, 1989.
- [10] A. Greenbaum and Z. Strakoš. Predicting the behavior of finite precision Lanczos and conjugate gradient computations. *SIAM J. Matrix Anal. Appl.*, 13(1):121–137, 1992.
- [11] M. R. Hestenes and E. Stiefel. Methods of conjugate gradients for solving linear systems. *J. Research Nat. Bur. Standards*, 49:409–436, 1952.
- [12] G. Meurant. The computation of bounds for the norm of the error in the conjugate gradient algorithm. *Numer. Algo.*, 16(1):77–87, 1998.
- [13] G. Meurant. Numerical experiments in computing bounds for the norm of the error in the preconditioned conjugate gradient algorithm. *Numer. Algo.*, 22(3-4):353–365, 1999.
- [14] G. Meurant. *The Lanczos and Conjugate Gradient Algorithms*, volume 19 of *Software, Environments, and Tools*. Society for Industrial and Applied Mathematics (SIAM), Philadelphia, PA, 2006.
- [15] G. Meurant. On prescribing the convergence behavior of the conjugate gradient algorithm. *Numer. Algorithms*, 84(4):1353–1380, 2020.
- [16] G. Meurant, J. Papež, and P. Tichý. Accurate error estimation in cg. *Numer. Algorithms*, 88(3):1337–1359, 2021.
- [17] G. Meurant and P. Tichý. On computing quadrature-based bounds for the  $A$ -norm of the error in conjugate gradients. *Numer. Algo.*, 62(2):163–191, 2013.
- [18] G. Meurant and P. Tichý. Erratum to: On computing quadrature-based bounds for the  $A$ -norm of the error in conjugate gradients [mr3011386]. *Numer. Algorithms*, 66(3):679–680, 2014.
- [19] G. Meurant and P. Tichý. Approximating the extreme Ritz values and upper bounds for the  $A$ -norm of the error in CG. *Numer. Algorithms*, 82(3):937–968, 2019.
- [20] D. P. O’Leary, Z. Strakoš, and P. Tichý. On sensitivity of Gauss-Christoffel quadrature. *Numer. Math.*, 107(1):147–174, 2007.
- [21] C. C. Paige. Accuracy and effectiveness of the Lanczos algorithm for the symmetric eigenproblem. *Linear Algebra Appl.*, 34:235–258, 1980.
- [22] B. N. Parlett. *The Symmetric Eigenvalue Problem*, volume 20 of *Classics in Applied Mathematics*. Society for Industrial and Applied Mathematics (SIAM), Philadelphia, PA, 1998. Corrected reprint of the 1980 original.
- [23] Z. Strakoš. On the real convergence rate of the conjugate gradient method. *Linear Algebra Appl.*, 154/156:535–549, 1991.
- [24] Z. Strakoš and P. Tichý. On error estimation in the conjugate gradient method and why it works in finite precision computations. *Electron. Trans. Numer. Anal.*, 13:56–80, 2002.
- [25] Z. Strakoš and P. Tichý. Error estimation in preconditioned conjugate gradients. *BIT*, 45(4):789–817, 2005.
- [26] D. Šimonová and P. Tichý. When does the Lanczos algorithm compute exactly? *Electron. Trans. Numer. Anal.*, 55:547–567, 2022.